Analytical description of physical librations of Saturnian coorbital satellites Janus and Epimetheus

Philippe Robutel, Nicolas Rambaux, Julie Castillo-Rogez

Analytical description of physical librations of Saturnian coorbital satellites Janus and Epimetheus

Philippe Robutel [a], Nicolas Rambaux [b, a], Julie Castillo-Rogez [c]

[a] *ASD, IMCCE-CNRS UMR8028, Observatoire de Paris, Paris, France*
[b] University Pierre et Marie Curie - Paris 6, France
[c] Jet Propulsion Laboratory, Caltech, Pasadena, USA

February 3, 2010

Abstract

Janus and Epimetheus are famously known for their distinctive horseshoe-shaped orbits resulting from a 1:1 orbital resonance. Every four years these two satellites swap their orbits by a few tens of kilometers as a result of their close encounter. Recently Tiscareno et al. (2009) have suggested a model of rotation based on images from the Cassini orbiter. Assuming that the satellites follow a Keplerian orbit outside the swap, these authors inferred the amplitude of librational motion in longitude at the orbital period. By using an orbital model that includes the orbital swap, we characterize how that event impacts the rotation of the satellites. To that purpose, we have developed a formalism based on quasi-periodic series with long- and short-period librations. In this framework, the amplitude of the libration at the orbital period is found proportional to a term accounting for the orbital swap, which was absent from previous studies. From this approach we highlight a large error in the libration amplitude when the swap is neglected. We checked the analytical quasi-periodic development by performing a numerical simulation and find both results in good agreement. Thus a robust determination of the librational motion of these satellites from observations requires to explicitly take into account the swap in the description of the orbital model.

1 Introduction

The orbital motion of Janus and Epimetheus presents a peculiar horseshoe-shaped orbit resulting from a 1:1 orbital resonance (e.g. Dermott and Murray 1981; Yoder et al. 1983 ; Murray and Dermott 1999; Jacobson et al. 2008 and references therein). Every four years the two satellites swap their orbits by of a few tens of kilometers as a result of their close encounter. As the mass of Janus is 3.6 times greater than the mass of Epimetheus, the dynamical motion of the latter is more sensitive to the swap than the dynamical motion of Janus.

The rotational motion of the satellites depends mainly on the gravitational torque of Saturn acting on the dynamical figure of each moon. The expression of the gravitational torque is:

$$\vec{T} = \frac{3GM}{r^3}\vec{u} \times [I]\vec{u} \tag{1}$$

with G the gravitational constant, M the mass of Saturn, $[I]$ the moment of inertia of the moon, r the distance between Saturn and the moon, and $\vec{u}$ the unit vector toward Saturn in the moon's reference frame. The gravitational torque $\vec{T}$ depends on the relative Saturn-moon distance, hence the swap also yields his signature on the rotational motion of the satellites.

First estimates of the rotational motion of the two coorbital satellites Janus and Epimetheus have been obtained by Tiscareno et al. (2009). From images provided by the Cassini orbiter, they fitted a numerical shape model of the moons, which included the amplitude of the libration in longitude at the orbital frequency. The libration in longitude corresponds to the oscillation of the body along its equatorial plane. Tiscareno et al. (2009) obtained an amplitude of $5.9° \pm 1.2°$ for Epimetheus. For Janus, the uncertainty on the fit of the libration determination is too large to yield an accurate librational amplitude. However, based on their shape model, Tiscareno *et al.* suggested a value of $0.33° \pm 0.06°$ for the amplitude of the libration in longitude. In addition, they identified an unexplained constant phase of 5.3° for Janus and of 1.0° for Epimetheus. A recent numerical study by Noyelles (2010) explored the three-dimensional rotational motion of these satellites based on the numerical shape deduced by Tis-

careno et al. (2009). Noyelle's study suggests a strong influence of the swap on the rotational motion of Janus and Epimetheus, which we propose to explore in the present study.

The orbital motion of Janus and Epimetheus appears to be very regular, at least over a timescale of several thousands of years. Thus, the trajectories of these satellites can be considered as quasi-periodic. Schematically these trajectories evolve on three different timescales. The shortest corresponds to the mean motion of the satellites with a period of about 0.7 days. The second component has a period of 8 years and is associated with the close encounters of the satellites. The long-period component is the secular variations of the satellites eccentricities and inclinations over periods of a few thousands years. Since the rotation of Janus and Epimetheus is synchronous with their orbital motion, it reflects these different timescales.

One of the goals of this paper is to understand the influence of the 8-year horseshoe motion on the librations of Janus and Epimetheus. To this purpose, we develop an analytical solution of the rotation of these bodies that can simulate the main features of their spin. First we recall the solution of the libration in longitude for a Keplerian orbit. Then, in Section 3, we model the orbits of the two satellites through quasi-periodic expansions. The fourth section is dedicated to the description of the librational motion of each satellite in co-orbital orbit. Finally in section 5, we compare these analytical developments against observational constraints.

2 Keplerian orbit

First, let us recall the librational response of a satellite in synchronous spin-orbit resonance with a fixed Keplerian orbit (constant semi-major axis a and eccentricity e). The position of the moon is determined through its relative distance with Saturn r, and its orbital longitude is defined by the draconic true longitude (angle between the body and its line of nodes) or mean anomaly ℓ. We neglect the effect of obliquity, which is small (Noyelles, 2010), so that the orientation of the body is only specified by the angle θ defined with respect to the line of nodes.

The dynamical equation governing the rotation of the moon is the angular momentum balance with the gravitational torque exerted by Saturn. It can be written as

$$\ddot{\gamma} + \frac{\sigma^2}{2}\left(\frac{a}{r}\right)^3 \sin 2(\ell + \gamma + \gamma_0 - v) = 0, \qquad (2)$$

where γ is the librational angle defined as $\gamma = \theta - \ell$ and γ_0 is the constant representing the initial value of γ located at the ascending node of the orbit. The frequency σ is the librational frequency of the spin-orbit resonance. It is equal to $\sigma^2 = 3n^2(B-A)/C$ where $A < B < C$ are the moment of inertia of the satellite and n its mean motion.

For a small eccentricity e, the difference between the true and the mean anomalies is approximated at first-order in e by $v - \ell = 2e\sin\ell + \omega$ where ω is the argument of the pericenter. In addition, we approximate $a = r$, and, for γ small, the linearized equation of Eq. (2) is

$$\ddot{\gamma} + \sigma^2\gamma = 2e\sigma^2 \sin\ell \qquad (3)$$

where $\omega = \gamma_0$ in order to have the librational angle oriented toward the central planet at the pericenter passage (e.g. Murray and Dermott 1999). The librational solution is then simply

$$\gamma = A_\gamma \sin(\sigma t + \phi_\gamma) + \frac{2e\sigma^2}{\sigma^2 - n^2}\sin\ell \qquad (4)$$

where A_γ, ϕ_γ depends on the initial conditions and the right-hand side term is the forced libration. The forced libration oscillates at the mean motion frequency, and its amplitude is proportional to the ratio of the eccentricity to the difference between the libration frequency σ and the forced frequency n. Therefore, the amplitude of the forced libration depends on both the magnitude of the torque and the proximity of the libration frequency to the orbital frequency.

In the following sections, we describe the orbits and investigate the impact of the horseshoe-shaped orbit on the physical librations.

3 Orbital description of Janus and Epimetheus

3.1 Osculating elliptical elements and fundamental frequencies

The co-orbital satellites Janus and Epimetheus are famously known to exchange their orbits every four years. This swap takes a short time-span, which does not exceed six months. In order to model the peculiar orbital motion of these satellites, we numerically integrate the three-body problem composed of Saturn, Janus, and Epimetheus, including the oblateness J_2 of Saturn. By using the frequency analysis developed by Laskar (1988, 2005) for the purpose of Celestial Mechanics studies, we express the numerical solution as a quasi-periodic function expanded in Fourier series, where each frequency is a linear combination (with integer coefficients) of six fundamental frequencies (proper frequencies) denoted by $(\bar{n}, \nu, g_J, g_E, s_J, s_E)$. The first of these frequencies, $\bar{n}$, called proper mean motion, is associated to the mean orbital motion common

Table 1: Fundamental frequencies characteristic of the Saturn-Janus-Epimetheus system. These frequencies are derived from a 400 years long numerical integration of the three-body problem including Saturn's oblateness.

	Freq. (rad/day)	Per.
$\bar{n}$	9.045924661	0.69459 (days)
ν	-0.002147268	8.01130 (yrs)
g_J	0.034948638	0.49222 (yrs)
g_E	0.034952058	0.49217 (yrs)
s_J	-0.034812320	0.49414 (yrs)
s_E	-0.034813195	0.49413 (yrs)

to the two co-orbital satellites, and it is constant along satellite orbits. In the same way, the five other proper frequencies are also constant and might be considered as integrals of movement (Laskar, 2005). The second fundamental frequency ν corresponds to the libration frequency along the horseshoe orbits, while the four last ones are associated to the motion of the pericenters (g_E, g_J) and of the ascending nodes (s_E, s_J).

If the gravitational interactions between Janus and Epimetheus were negligible, then the relations $g_J = g_E$ and $s_J = s_E$ would be satisfied, and the eccentricities and inclinations of the two satellites would be constant (excepted for small short-period variations). However, due to the mutual satellites interactions, the proper frequencies of precessions of the orbits are slightly different, and both eccentricities and inclinations undergo large long-term variations with frequencies equal to $g_J - g_E$ and $s_J - s_E$. The corresponding periods are about 4850 and 25000 years, respectively. The long-term variations of the eccentricities will be neglected in the present work. Their impact on the rotation of the co-orbital satellites is mentioned in section 5.2.

The initial conditions of the numerical integrations come from the ephemeris *Horizons* (Giorgini et al., 1996). The model used in the ephemeris *Horizons* takes into account the gravitational interactions with the Sun and the other main satellites of the Saturnian system (Jacobson et al., 2008). Thus, in order to be consistent with that model, we fit the initial conditions of our integration in such a way that the fundamental frequencies $\bar{n}$ and ν are the same in both cases. The entire set of fundamental frequencies, as well as their associated periods, are displayed in Table 1.

Due to the high orbital precession rate generated by Saturn's oblateness, we define the elliptic elements by introducing Saturn's J_2 in the third Kepler's law, which yields:

$$n^2 a^3 = \mu, \quad \text{with}$$
$$\mu = G(m_S + m_J + M)\left(1 + \frac{3}{2} J_2 \left(\frac{R}{\bar{a}}\right)^2\right) \tag{5}$$

where M, R are the mass and equatorial radius of Saturn, m_J, m_E the masses of Janus and Epimetheus (in the following, we use the subscript J for Janus and E for Epimetheus), and $\bar{a}$ the above-mentioned semi-major axis barycenter of Janus and Epimetheus. The elliptic elements $(a, e, I, \lambda, \varpi, \Omega)$[1] are then deduced from the planetocentric positions and velocities of the satellites. As shown by Figure 1, this definition of elliptic elements removes the main orbital oscillations from the elliptical elements (Greenberg, 1981). In addition, changing the value of μ shifts the mean value of the semi-major axis by a quantity of the order of $J_2(R_S/\bar{a})^2$, which leads to the translation of about 600 km clearly visible in Fig. 1.

3.2 Analytical expression of the elliptic elements' variations

In this section, we detail the quasi-periodic expansion of the elliptic elements for both satellites that will be useful for the rotation study.

According to classical theories (i.e Dermott and Murray 1981; Yoder et al. 1983 or Namouni 1999, for more recent developments), the variations of the mean longitudes and semi-major axes of the coorbital satellites are accurately approximated by the expressions:

$$\begin{aligned} \lambda_J &\approx \lambda^{(0)} + \bar{n}t + \zeta_E \lambda_r \bmod(2\pi) \\ \lambda_E &\approx \lambda^{(0)} + \bar{n}t - \zeta_J \lambda_r \bmod(2\pi) \end{aligned} \tag{6}$$

$$\begin{aligned} a_J &\approx \bar{a} + \zeta_E a_r \\ a_E &\approx \bar{a} - \zeta_J a_r \end{aligned} \tag{7}$$

where $\zeta_J = m_J/(m_J + m_E)$ and $\zeta_E = 1 - \zeta_J$. The variables a_r and λ_r represent the relative semi-major axes and mean longitudes of the satellites, that is: $a_r = a_J - a_E$ and $\lambda_r = \lambda_J - \lambda_E$. These relations clearly reflect the symmetries between the orbits of Janus and Epimetheus. Formula (7) implies that the barycenter of the semi-major axes, namely $\zeta_J a_J + \zeta_E a_E$, is almost constant[2]. Numerical simulation shows that the relative variation of this

[1] The index "J" or "E" is added to specify that the elements are related to Janus or Epimetheus if necessary.

[2] Once averaged the Hamiltonian of the three-body problem on the mean longitude of the satellites, the quantity $\zeta_J\sqrt{a_J} + \zeta_E\sqrt{a_E}$ becomes an integral of the motion. The relative semi-major axis a_r remaining always very small with respect to a_J and a_E, the stated property holds.

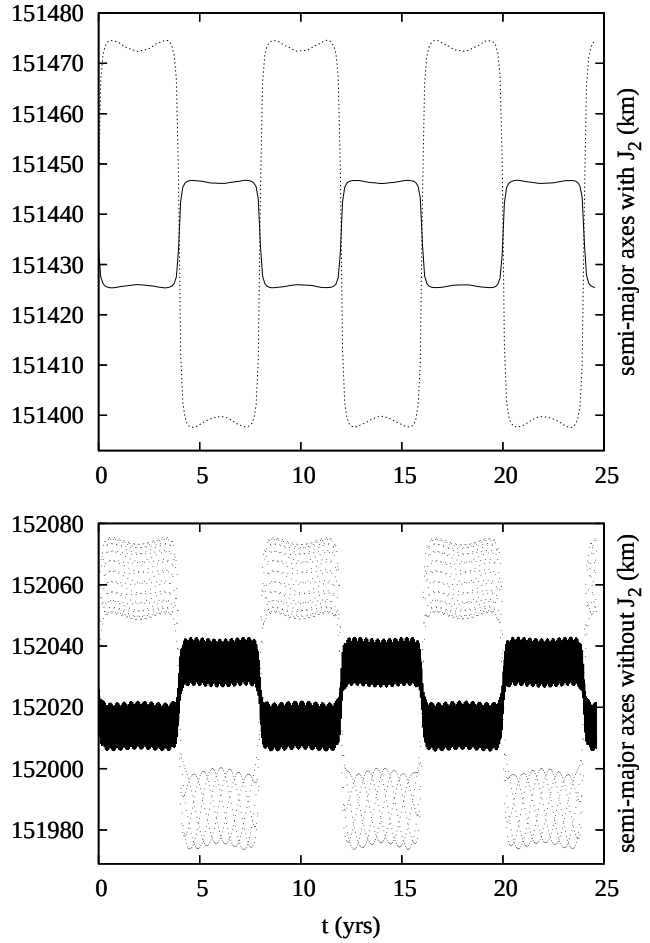

Figure 1: Variation of the semi-major axis of Janus and Epimetheus: the upper plot shows the temporal variations of the semi-major axes of the two satellites (solid line for Janus and dotted line for Epimetheus), when J_2 is included in the third Kepler's law. The semi-major axes oscillate around the mean value $\bar{a} = 151436.9$ km. When J_2 is not considered (bottom plot), large short-period oscillations are superimposed to the above-mentioned 8-years signal. The signals are periodic with periods of $2\pi/\nu \approx 8$ years. In the last case, the value of $\bar{a}$ is equal to 152024.4 km, which is about 600 km higher than when J_2 is taken into account.

quantity is smaller than $2\,10^{-7}$ if Saturn's oblateness is included in the definition of the elliptic elements, while the variation is about 200 times more without J_2. Similarly, formula (6) implies that the barycenter of the mean longitudes $\zeta_J\lambda_J + \zeta_E\lambda_E$ is almost only affected by variations directly proportional to the time. In other words, $\frac{d}{dt}\left(\zeta_J\lambda_J + \zeta_E\lambda_E\right) \approx \bar{n}$. It turns out that the main variations of a and λ are given by the relative motion in coordinates (a_r, λ_r).

Neglecting the terms of powers greater than two in eccentricities (which are very small for these satellites), the relative motion of the satellites satisfies the differential system:

$$\left\{\begin{array}{lll} \dot{a}_r & = 2\varepsilon\bar{n}\bar{a}\,\left(1-(2-2\cos\lambda_r)^{-3/2}\right)\sin\lambda_r \\ \dot{\lambda}_r & = -\dfrac{3\bar{n}}{2}\dfrac{a_r}{\bar{a}}, \quad \text{with} \quad \varepsilon = \dfrac{m_J+m_E}{M+m_J+m_E} \end{array}\right. \tag{8}$$

The solutions of these equations can be expanded in a Fourier series as:

$$a_r(t) = \bar{a}\left[\sum_{p\geq 1}\alpha_p^{(r)}\cos\left(p\nu t+\varphi_p^{(r)}\right)\right] \quad \text{with} \quad \alpha_{2n}^{(r)} = 0 \tag{9}$$

$$\lambda_r(t) = \pi + \sum_{p\geq 1}\beta_p^{(r)}\sin\left(p\nu t+\varphi_p^{(r)}\right) \quad \text{with} \quad \beta_{2n}^{(r)} = 0 \tag{10}$$

where ν is the frequency of the relative motion, that is the second fundamental frequency defined in Section 3.1. It corresponds to a period of eight years for Janus and Epimetheus. The vanishing of the even coefficients in the series (9) and (10) is due to the symmetries of the system (8). Indeed, the invariance of the differential system by the transformation $z \longmapsto -z$ where $z = (a_r, \lambda_r)$, leads to the relations $z(t + T/2) = -z(t)$, where $T = 2\pi/\nu$ is the period of the solution. Applying this relation to the Fourier expansion of z we obtain $\alpha_{2n}^{(r)} = \beta_{2n}^{(r)} = 0$.

While the differential system (8) is integrable, it is hard to get an analytical expansion of its solutions in the form of a Fourier series. Consequently, the coefficients $\alpha_p^{(r)}$, $\beta_p^{(r)}$ and the phases $\varphi_p^{(r)}$ have been inferred from the solutions of the numerical integration. A truncated expression of this expansion is given in Table 2. The comparison between the third and fourth columns, which display the coefficients $\alpha_p^{(r)}$ and $\beta_p^{(r)}$, respectively, emphasizes the different decreasing speed of theses sequences. While the coefficients of the relative semi-majors axis seem to decrease slowly, the sequence $\beta_p^{(r)}$ converges more rapidly. Indeed , Equation (8) imposes the coefficients $\beta_p^{(r)}$ to be proportional to $p^{-1}\alpha_p^{(r)}$.

In order to illustrate the convergence of the series (9) and (10) towards the solution of the equation of relative motion (8), we consider different approximations of these series for which the N first terms are summed. To the relative orbit of the two coorbital satellites in the plan (a_r, λ_r) visible in Fig. 2 (bold curve), are superimposed the approximated orbit (dashed curves) obtained by varying the integer N. The ellipse obtained for $N = 1$ provides a very crude approximation of the relative orbit, while the

approximation generated at $N = 30$ starts matching accurately the numerical solution. In addition to the central symmetry $z \longmapsto -z$ mentioned above, Fig. 2 emphasizes a second symmetry with respect to the axis of coordinates. These symmetries impose relationships between the phases φ_p, whose description is beyond the scope of this paper.

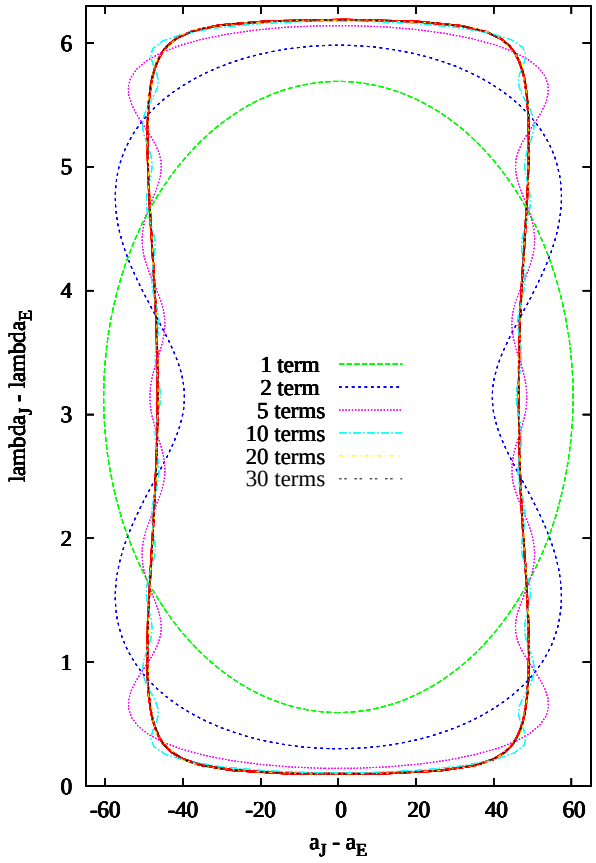

Figure 2: Relative orbit of the satellites: the X-axis represents the relative semi-major axis $a_r = a_J - a_E$ in km, while the Y-axis corresponds to the relative mean longitude $\lambda_r = \lambda_J - \lambda_E$ in radians. The solid red curve plots the orbit deduced from the numerical simulations, while the dotted curves stands for several approximation given by formulas (9) and (10). See text for more details.

Finally, from the periodic representations (9) and (10) of the quantity $z(t) = (a_r(t), \lambda_r(t))$ and according to formulas (6) and (7), the trigonometric approximations of the semi-major axis and mean longitude of the satellites read:

$$\begin{aligned} a^{(x)}(t) &= \bar{a}\left[1 + \sum_{1\le p\le N} \alpha_p^{(x)} \cos\left(p\nu t + \varphi_p^{(x)}\right)\right] \\ &= \bar{a}\left[1 + \mathcal{A}_N^{(x)}\right] \end{aligned} \tag{11}$$

$$\begin{aligned} \lambda^{(x)}(t) &= \lambda_0 + \bar{n}t + \sum_{1\le p\le N} \beta_p^{(x)} \sin\left(p\nu t + \varphi_p^{(x)}\right) \\ &= \lambda_0 + \bar{n}t + \mathcal{B}_N^{(x)} \end{aligned} \tag{12}$$

$$\begin{aligned} &\alpha_p^{(x)} = (1-\zeta_x)\alpha_p^{(r)}, \quad \beta_p^{(x)} = (1-\zeta_x)\beta_p^{(r)}, \\ &\varphi_p^{(J)} = \varphi_p^{(r)}, \quad \varphi_p^{(E)} = \varphi_p^{(r)} + \pi \end{aligned} \tag{13}$$

where the index x replaces J and E, whether we consider Janus or Epimetheus. The numerical values of the coefficients $\alpha_p^{(x)}$ and $\beta_p^{(x)}$ are reported in the fifth and sixth columns of Table 2 for Janus and in the seventh and eighth columns for Epimetheus. In addition, the ratios of each $\alpha_p^{(E)}/\alpha_p^{(J)}$ to $\beta_p^{(E)}/\beta_p^{(J)}$ listed in Table 2 are close to 3.6, in agreement with the formulae (13). The short-period oscillations do not appear in that table because they are negligible in comparison to the other parameters.

In the following section, we use this representation of the elliptical elements of the satellites, especially for the mean longitudes, to develop an elementary perturbation theory describing the rotation of Janus and Epimetheus. We consider in the next section that the eccentricities and inclinations are constant, as underlined in section 3.1. In the same way, the precession of the pericenters and nodes will be approximated by assuming uniform motion defined as:

$$e(t) = \bar{e}, \quad \varpi(t) = gt + \varpi_0 \tag{14}$$

$$I(t) = \bar{I}, \quad \Omega(t) = st + \Omega_0 \tag{15}$$

4 Physical librations

4.1 Perturbative analysis

4.1.1 Dynamical equations

The equation governing the physical libration is inferred from the angular momentum balance equation projected onto the equatorial plane of the body

$$C\ddot{\theta} - \frac{3(B-A)}{2}\frac{Gm}{r^3}\sin 2(v-\theta) = 0 \tag{16}$$

p	Frequency (rad/day)	$\bar{a}\alpha_p^{(r)}$ (km)	$\beta_p^{(r)}$ (rad)	$\bar{a}\alpha_p^{(J)}$ (km)	$\beta_p^{(J)}$ (rad)	$\bar{a}\alpha_p^{(E)}$ (km)	$\beta_p^{(E)}$ (rad)	$\varphi_p^{(r)}$ (rad)
1	-2.14726e-3	60.4335555	2.5479054	13.1270068	0.5534404	47.3065487	1.9944650	-1.5835210
3	-6.44180e-3	20.8015755	0.2923293	4.5183908	0.0634980	16.2831847	0.2288313	-1.6089568
5	-1.07363e-2	11.0167392	0.0929054	2.3929886	0.0201803	8.6237506	0.0727251	-1.6344092
7	-1.50308e-2	7.0984885	0.0427538	1.5418902	0.0092867	5.5565983	0.0334671	-1.6609244
9	-1.93254e-2	4.9877777	0.0233653	1.0834145	0.0050753	3.9043632	0.0182900	-1.6866709
11	-2.36199e-2	3.6827072	0.0141150	0.7999351	0.0030660	2.8827721	0.0110490	-1.7124149
13	-2.79144e-2	2.8083507	0.0091078	0.6100127	0.0019783	2.1983379	0.0071295	-1.7381559
15	-3.22090e-2	2.1908244	0.0061577	0.4758775	0.0013375	1.7149470	0.0048202	-1.7638937
17	-3.65035e-2	1.7381554	0.0043107	0.3775515	0.0009363	1.3606040	0.0033743	-1.7896277
19	-4.07981e-2	1.3970712	0.0031001	0.3034633	0.0006734	1.0936080	0.0024267	-1.8153577
21	-4.50926e-2	1.1345829	0.0022778	0.2464472	0.0004948	0.8881358	0.0017831	-1.8410832
23	-4.93871e-2	0.9291897	0.0017033	0.2018329	0.0003700	0.7273568	0.0013333	-1.8668040
25	-5.36817e-2	0.7663012	0.0012923	0.1664513	0.0002807	0.5998499	0.0010116	-1.8925195
27	-5.79762e-2	0.6356894	0.0009926	0.1380806	0.0002156	0.4976089	0.0007770	-1.9182293
29	-6.22708e-2	0.5299910	0.0007705	0.1151214	0.0001674	0.4148696	0.0006031	-1.9439331
31	-6.65653e-2	0.4437859	0.0006035	0.0963965	0.0001311	0.3473895	0.0004725	-1.9696303
33	-7.08598e-2	0.3730099	0.0004765	0.0810229	0.0001035	0.2919870	0.0003730	-1.9953207
35	-7.51544e-2	0.3145665	0.0003789	0.0683282	0.0000823	0.2462383	0.0002966	-2.0210036
37	-7.94489e-2	0.2660642	0.0003032	0.0577928	0.0000659	0.2082713	0.0002373	-2.0466787
39	-8.37434e-2	0.2256343	0.0002439	0.0490109	0.0000530	0.1766234	0.0001909	-2.0723454
41	-8.80380e-2	0.1918019	0.0001972	0.0416620	0.0000428	0.1501398	0.0001544	-2.0980031
43	-9.23325e-2	0.1633917	0.0001602	0.0354909	0.0000348	0.1279007	0.0001254	-2.1236514
45	-9.66271e-2	0.1394605	0.0001307	0.0302927	0.0000284	0.1091677	0.0001023	-2.1492896
47	-1.00921e-1	0.1192455	0.0001070	0.0259018	0.0000232	0.0933437	0.0000837	-2.1749173
49	-1.05216e-1	0.1021264	0.0000879	0.0221833	0.0000191	0.0799432	0.0000688	-2.2005337
51	-1.09510e-1	0.0875956	0.0000724	0.0190270	0.0000157	0.0685686	0.0000567	-2.2261383
53	-1.13805e-1	0.0752358	0.0000598	0.0163423	0.0000130	0.0588936	0.0000468	-2.2517303
55	-1.18099e-1	0.0647024	0.0000496	0.0140543	0.0000108	0.0506481	0.0000388	-2.2773095

Table 2: Periodic approximation of the semi-major axes of Janus and Epimetheus. The relative quantities a_r and λ_r according to (9) and (10) are represented in the third and fourth columns. The sixth and seventh columns contain the coefficients of $a^{(J)}$ and $\lambda^{(J)}$ appearing in (11) and (12), while the eighth and ninth columns correspond to the same quantities for Epimetheus. The frequencies listed in the second column are equal to $p\nu$ where p is in the first column. The origin of time in formulas (9) is equal to 1949-Dec-28 00:00:00.0000 from the ephemeris *Horizons*.

where all variables have been defined in Section 2. Since the angle $v-\theta$ remains always small, the linearization of the equation (16) is a valid approximation to the rotation. Therefore, in this section, we will consider the linear time-dependent equation:

$$\ddot{\theta}+\sigma^2\left(\frac{a}{r}\right)^3(\theta-v)=0, \quad \text{with } \sigma^2=3\frac{Gm}{a^3}\frac{(B-A)}{C} \quad (17)$$

This equation is not integrable because the quantities σ, a/r and v are implicit functions of time. However, the elliptic elements of the satellites are quasi-periodic functions of time, so that it becomes possible to get an approximated solution of this equation using an elementary perturbation theory, as was done in section 3 for the orbit.

Let us first introduce the physical libration γ. This angle is defined as the oscillation of θ around the uniform motion $(\bar{n}-s)t$, where $\bar{n}-s$ is the main frequency of the angle $\lambda-\Omega$. Therefore the physical libration reads: $\gamma=\theta-(\bar{n}-s)t-\gamma_0$, the angle γ_0 is such that $\gamma=0$ at the pericenter of the orbit. Consequently, using the relation (12), the angle $\theta-v$ also reads:

$$\begin{aligned}\theta-v&=\gamma-v+(\bar{n}-s)t+\gamma_0\\&=\gamma-[\ell+\omega-(\bar{n}-s)t-\gamma_0]-[f-\ell]\\&=\gamma-\mathcal{B}_N-2e\sin\ell\end{aligned} \quad (18)$$

where terms of order 2 and greater in eccentricity have been neglected. At this point, it is convenient to use the function $y=\gamma-\mathcal{B}_N$, where $\mathcal{B}_N=\ell+\omega-(\bar{n}-s)t-\gamma_0$ is presented in previous sections. Indeed, although the amplitudes of the terms contained in $\mathcal{B}_N$ are very large, their frequencies are small and therefore the acceleration generated by $\mathcal{B}_N$, which is of order ν^2, is negligible with respect to σ^2. Under these approximations, Equation (17) becomes:

$$\ddot{y}+\sigma^2\left(\frac{a}{r}\right)^3 y=2e\sigma^2\left(\frac{a}{r}\right)^3\sin\ell \quad (19)$$

This equation has the same form as in the Keplerian case (see section 2), but it depends quasi-periodically on the time because, according to formula (12), ℓ reads:

$$\ell=\lambda-\varpi=\lambda_0-\varpi_0+(\bar{n}-g)t+\mathcal{B}_N \quad (20)$$

so

$$\begin{aligned}e^{i\ell}&=e^{i\ell_0}e^{i(\bar{n}-g)t}\prod_{1\le q\le N}e^{i\beta_q\sin(q\nu t+\varphi_q)}\\&=e^{i\ell_0}e^{i(\bar{n}-g)t}\prod_{1\le q\le N}\sum_{k\in Z}J_k(\beta_q)e^{ik(q\nu t+\varphi_q)}\end{aligned} \quad (21)$$

where the $J_k(x)$ are the Bessel functions (see Appendix A). It is important to keep in mind that the coefficients β_q vanish for even values of q. Applying usual properties of the Bessel functions that are recalled in Appendix A, we deduce that, for q odd, the ratio between the coefficients $J_k(\beta_q)$ computed for Epimetheus and for Janus is well approximated by:

$$\left|\frac{J_k(\beta_q^{(E)})}{J_k(\beta_q^{(J)})}\right|\approx\left(\frac{\zeta_J}{\zeta_E}\right)^{|k|}\approx 3.6^{|k|} \quad (22)$$

For this reason, the coefficients of the expansion (21) decrease much more rapidly for Janus than for Epimetheus. Consequently, the number of terms necessary to approximate $e^{i\ell}$ to a given accuracy using a truncated expression of (21) is different for the two moons. For the following, we set $N=1$ and limit the expansion over k to order N' (the implications of these simplifications on the accuracy of the analytical representation of the rotation is discussed in Section 4.2). Then we have:

$$e^{i\ell}=e^{i\ell_0}e^{i(\bar{n}-g)t}\sum_{|k|\le N'}J_k(\beta_1)e^{ik(\nu t+\varphi_1)} \quad (23)$$

It turns out that, under these approximations and assuming as in (14) that the eccentricity is constant and denoted $\bar{e}$:

$$\begin{aligned}&e\sin\ell=\bar{e}\mathcal{S}_{N'}\quad\text{with}\\&\mathcal{S}_{N'}=\quad J_0(\beta_1)\sin((\bar{n}-g)t+\ell_0)+\\&\sum_{p\le N'}J_p(\beta_1)\big[(\sin((\bar{n}-g+p\nu)t+p\varphi_1+\ell_0)+\\&\qquad(-1)^p\sin((\bar{n}-g-p\nu)t-p\varphi_1+\ell_0)\big]\end{aligned} \quad (24)$$

where N' is an arbitrary integer. Using (23) we also get the expression of:

$$\left(\frac{a}{r}\right)^3=1+3\bar{e}\mathcal{C}_{N''} \quad (25)$$

The expression of $\mathcal{C}_N$ is the same as $\mathcal{S}_N$, where sine functions are replaced by cosine functions. The last term that we have to expand is σ^2. By (11) with $N=1$, we have:

$$\sigma^2\approx\bar{\sigma}^2(1-3\mathcal{A}_1)\quad\text{with}\quad\bar{\sigma}^2=3\frac{Gm}{\bar{a}^3}\frac{B-A}{C} \quad (26)$$

By substitution of the relations (24), (25) and (26) in the (19) this equation becomes:

$$\ddot{y}+\bar{\sigma}^2(1-3\mathcal{A}_1)(1+3\bar{e}\mathcal{C}_{N''})y=2\bar{e}\bar{\sigma}^2(1-3\mathcal{A}_1)\mathcal{S}_{N'} \quad (27)$$

If we split y into a sum of terms of decreasing magnitude as $y=y_0+y_1+\cdots$, we obtain the following system of equations:

$$\ddot{y}_0+\bar{\sigma}^2y_0=2\bar{e}\bar{\sigma}^2\mathcal{S}_{N'} \quad (28)$$

$$\ddot{y}_1+\bar{\sigma}^2y_1=3\bar{\sigma}^2(\mathcal{A}_1-\bar{e}\mathcal{C}_{N''})y_0-6\bar{e}\bar{\sigma}^2\mathcal{A}_1\mathcal{S}_{N'} \quad (29)$$

$$\vdots$$

The solutions of these equations are trigonometric sums, whose frequencies are linear combinations with integer coefficients of fundamental frequencies of the satellites $(\bar{n}, \nu, g, s)$ and of the eigenfrequency $\bar{\sigma}$. In the presence of dissipation, the solution of the motion is rapidly damped and tends to an asymptotic quasi-periodic solution whose frequencies are independent of $\bar{\sigma}$. This solution, usually called "forced solution," is studied in Section 4.1.2. Although the part of the solution that depends on the eigenfrequency $\bar{\sigma}$ (that we call libration of proper frequency) is probably not present in the current rotation of Janus and Epimetheus, it is worth studying briefly. Section 4.1.3 is devoted to this question.

4.1.2 Forced librations

To begin with, let us associate to a quasi-periodic function f the function $\hat{f}$ such that:

$$\text{if} \quad f(t) = \sum_p f_p \sin(v_p t + \phi_p)$$

$$\text{then} \quad \hat{f}(t) = \sum_p \frac{\bar{\sigma}^2}{\bar{\sigma}^2 - v_p^2} f_p \sin(v_p t + \phi_p)$$

With these notations, the general solution of (28) reads:

$$y_0(t) = h \sin(\bar{\sigma} t + \psi) + 2\bar{e}\hat{S}_{N'} \tag{30}$$

where h and ψ are arbitrary constants. In this section, we focus on the forced solution, so $h = 0$. As a consequence, It is easy to verify in (28) that the contribution of $\bar{e}y_0\mathcal{C}_{N''}$, denoted $\bar{e}\widehat{y_0\mathcal{C}_{N''}}$, is a second-order in eccentricity, and that $\bar{e}\widehat{\mathcal{A}_1 y_0}$ and $\bar{e}\widehat{\mathcal{A}_1\mathcal{S}_{N'}}$ are of order $\bar{e}\alpha_1$. As, for Janus and Epimetheus, the coefficient α_1 is lower than $\bar{e}$, then the term y_1 can be neglected. Finally, the forced libration can be approximated by the expression:

$$\begin{aligned}\gamma = &\sum_{1\le p\le N} \beta_p \sin(p\nu t + \varphi_p) \\ &+ \frac{2\bar{e}\bar{\sigma}^2 J_0(\beta_1)}{\bar{\sigma}^2 - (\bar{n}-g)^2} \sin((\bar{n}-g)t + \ell_0) + \\ &2\bar{e}\bar{\sigma}^2 \sum_{1\le p\le N'} J_p(\beta_1) \left[\frac{\sin((\bar{n}-g+p\nu)t + p\varphi_1 + \ell_0)}{\bar{\sigma}^2 - (\bar{n}-g+p\nu)^2} - \right. \\ &\left. (-1)^p \frac{\sin((\bar{n}-g-p\nu)t - p\varphi_1 + \ell_0)}{\bar{\sigma}^2 - (\bar{n}-g-p\nu)^2} \right]\end{aligned} \tag{31}$$

The librational angle γ is split in two types of terms exhibiting different behaviors. The first type corresponds to the $2\pi/\nu$-periodic terms that depend only on the coefficients β_p, i.e., on the mean longitudes of the satellites. For these long-period terms the dynamical figure has no influence. The second type includes terms that vary rapidly (quasi-periodic with short frequencies $\bar{n} - g \pm p\nu$) and depend on the triaxiality of the body $(B-A)/C$ through the libration proper frequency $\bar{\sigma}$.

The amplitudes of the rapidly oscillating terms depends on the magnitude of the forcing, $2\bar{e}J_p(\beta_1)$ and on the proximity of the forcing frequency $\bar{n} - g \pm p\nu$ with the libration proper frequency $\bar{\sigma}$. In the case of Janus, the proper frequency is 4.96 rad/day, which is far from the resonance, whereas for Epimetheus the proper frequency is equal to 8.52 rad/days, and its influence on the amplitude is substantial.

By contrast to the Keplerian case, the swap results in the amplitude of the term associated to the frequency $\bar{n} - g$ to be proportional to $J_0(\beta_1)$. This term is of the order of 1 for Janus, but it is significant in the case of Epimetheus as close to 0.22. Therefore, for both satellites, the rotation significantly departs from the Keplerian case.

4.1.3 Spin-orbit resonant libration

In this section we investigate the proper libration of the moons (also called free libration) and we especially focus on the influence of a small divisor on the solution. To this aim, let us remove the external forcing by imposing $\bar{e} = 0$ in (28) and (29). Then, the solution (30) reads $y_0(t) = h\sin(\bar{\sigma}t + \psi)$, where the amplitude h is small but different from zero. Consequently, by substitution of y_0 in the equation (29), we get:

$$\begin{aligned} y_1 = &\frac{3\bar{\sigma}^2\alpha_1 h}{2} \left(\frac{\sin((\nu+\bar{\sigma})t + \varphi_1 + \psi)}{\bar{\sigma}^2 - (\nu+\bar{\sigma})^2} - \right. \\ &\left. \frac{\sin((\nu-\bar{\sigma})t + \varphi_1 - \psi)}{\bar{\sigma}^2 - (\nu-\bar{\sigma})^2} \right) \\ = &-\frac{3}{2}\frac{\bar{\sigma}\alpha_1}{\nu} h \left(\sin(\nu t + \varphi_1)\cos(\bar{\sigma}t + \psi) + O(\frac{\nu}{\bar{\sigma}}) \right) \end{aligned} \tag{32}$$

In the previous section, the term $\mathcal{A}_1$ has been neglected since α_1 is very small (see Table 2). However, in the present situation, that term is multiplied by the factor $\bar{\sigma}/\nu$, which is about 2200 for Janus and 3700 for Epimetheus. Thus it generates a second-order solution y_1, whose size is comparable to the solution of order one y_0. Then, using the values of $\bar{\sigma}$ given in Table 3 for Janus and Epimetheus, the librational responses for the two satellites are:

$$y_J = h\left(\sin(\sigma t + \psi) + 0.3\sin(\nu t + \varphi_1)\cos(\bar{\sigma}t + \psi)\right) \tag{33}$$

$$y_E = h\left(\sin(\sigma t + \psi) + 1.87\sin(\nu t + \varphi_1)\cos(\bar{\sigma}t + \psi)\right) \tag{34}$$

The proper librations are combinations of a sine term with a constant amplitude and a cosine term with an amplitude

varying at the swap frequency. For Janus, the main term is the sine component, whereas for Epimetheus, it is the cosine component.

4.2 Comparison to a numerical study

In order to estimate the accuracy of the analytical solutions developed in the previous section, we compare our results to those of a numerical simulation of the rotational motion of the satellites. Starting from the numerical integration of the orbital motions described in Section 3, we introduce the dynamical equations (16), and we use some of the satellites physical properties listed in Table 3.

In order to clearly separate in the frequency analysis the frequencies $(\bar{n} - g \pm p\nu)$, which are quite close, we have to integrate the trajectories over a long time-span of about 400 years. On this long time-interval the eccentricities vary a lot due to gravitational interactions between the two satellites (see Fig. 4). In parallel, the analytical libration depends on the value of $\bar{e}$. For the sake of comparing the analytical and numerical solutions, we perform these calculations using the same mean value of e obtained over the 400-year interval, i.e. $\bar{e}_J = 0.007473$ and $\bar{e}_E = 0.007866$ (see Section 5.2). The results of the comparison are reported in Tables 4 and 5. These tables describe both the numerical and the analytical solutions for the librations in longitude γ for Janus (Table 4) and for Epimetheus (Table 5). The solutions are given in the form:

$$\begin{aligned} \gamma(t) &= \sum_p \gamma_p \sin(f_p t + \psi_p) \\ \text{with} \quad f_p &= j_p(\bar{n} - g) + k_p \nu \end{aligned} \tag{35}$$

The first and second columns contain the amplitudes of γ_p from the numerical simulation and the analytical expression (31). The third column contains the frequencies f_p, while the integers j_p and k_p are displayed in the fourth and fifth columns. The last column presents the phases ψ_p computed from the frequency analysis.

For the first column of Table 4 describing the libration of Janus, the four main librations result from the swap of its orbit (term $\mathcal{B}_N$). Then the term at the orbital period appears in the fifth position. The amplitude of the libration in longitude is 0.31°, which is 100 times smaller than the main term due to the swap, equal to 32°.

For Janus, columns one and two show a good agreement between the analytical and the numerical calculations. For those long-period terms that come from $\mathcal{B}_N$, the discrepancy between the analytical and numerical solution is smaller than 1%. By contrast, the accuracy of the short-period terms is a function of the considered harmonic, whose frequency is $\bar{n} - g \pm p\nu$. For $p = 0$, the discrepancy is about 1% and increases for increasing p, e.g. 19% for $p = 2$. This lack of accuracy can be ascribed to neglecting the terms β_q for q greater than three in the expansion (21), and consequently in the analytical solutions of the rotation (31). Indeed, as can be shown by a straightforward calculation, the amplitudes of the terms that have been neglected are given by $2J_3(\beta_1)J_1(\beta_3) \approx 2\,10^{-4}$ for $p = 0$, $J_2(\beta_1)J_1(\beta_3) \approx 4\,10^{-3}$ for $p = 1$ and $J_1(\beta_1)J_1(\beta_3) \approx 2\,10^{-1}$ for $p = 2$. These numerical values, which are deduced from Table 6, are in good agreement with the level of accuracy mentioned above.

The librational behavior of Epimetheus is reported in Table 5. Like for Janus, the main Epimetheus' librations are related to the orbital swap $\mathcal{B}_N$. However, contrarily to Janus, the amplitudes of the short-period terms at $\bar{n} - g \pm \nu$ and $\bar{n} - g \pm 2\nu$ are greater than the terms at $\bar{n} - g$. This is due to the fact that $J_1(\beta_1) > J_2(\beta_1) > J_0(\beta_1)$ for Epimetheus, while the relation $J_0(\beta_1) > J_1(\beta_1) > J_2(\beta_1)$ holds for Janus (see Tables 6 and 7). From comparing the first two columns of Table 5 we find that the accuracy on the short-period terms obtained for Epimetheus is worse than in the case of Janus. It reaches 5% for the three short-period terms and increases to 25% for $p = 4$, and even greater for $p = 5$. As for Janus, the accuracy of the analytical solution would be increased if the terms related to β_3 and possibly to β_5 were taken into account.

5 Discussion

5.1 Amplitude of libration at the orbital period

Tiscareno et al. (2009) deduced from images obtained by the *Cassini* Orbiter the shape triaxiality and the librational amplitude for both Epimetheus and Janus. The fitting approach used by these authors did not include the effect of the swap on the satellites rotation and assumed that the orbital segments outside the swap follow a purely Keplerian orbit. These authors superposed to a uniform rotation model a periodic term at the orbital period that accounts for the physical librations. The resulting libration solution is summarized in Section 2. These authors determined an amplitude of libration for Epimetheus of about 5.9° and estimated that of Janus to be of the order of 0.3°.

In the present study, we have taken into account the effect of the swap on the satellites orbits and expanded the librational motion of the moons as a quasi-periodic motion. According to the analytical solution developed in section 4, the ratio of the librational amplitudes at the orbital frequency computed from a Keplerian approach

Table 3: Physical properties of Janus and Epimetheus. (1) Porco *et al.* (2006), (2) Tiscareno et al. (2009).

	Janus	Epimetheus
Mean Radius (km)	89.4 ± 3	56.7 ± 3.1
Shape[(1)] (km)	193x173x137	135x108x105
Density (g/cm3)	0.64 ± 0.06	0.69 ± 0.11
Equ. Surf. Gravity (m/s2)	0.0137	∼0.0078
Central Pressure (MPa)	0.45	0.22
$\frac{(B-A)}{C}$ [(2)]	0.100	0.296
$\bar{\sigma}$ (rad/day)	4.95508166	8.52504483

Table 4: Frequency analysis in the librational motion of Janus.

Amp num (rad)	Amp ana (rad)	Freq (rad/days)	$\bar{n} - g_J$	ν	phase num (rad)
0.5583948	0.5534405	-2.147269e-3	0	1	-1.583713
0.0640676	0.0634981	-6.441806e-3	0	3	-1.609542
0.0203581	0.0201804	-1.073634e-2	0	5	-1.635363
0.0093699	0.0092868	-1.503088e-2	0	7	-1.661180
0.0060570	0.0059903	9.010976	1	0	-1.686992
0.0051208	0.0050754	-1.932542e-2	0	9	1.229299
0.0030935	0.0030661	-2.361995e-2	0	11	-1.738600
0.0019962	0.0019784	-2.791449e-2	0	13	-1.764395
0.0017190	0.0017257	9.008829	1	1	-1.790184
0.0017173	0.0017233	9.013123	1	-1	-1.815967
0.0013496	0.0013376	-3.220903e-2	0	15	1.454671
0.0009448	0.0009364	-3.650356e-2	0	17	-1.841743
0.0006795	0.0006734	-4.079810e-2	0	19	-1.867513
0.0004993	0.0004948	-4.509264e-2	0	21	-1.550684
0.0003734	0.0003700	-4.938717e-2	0	23	-3.133633
0.0002986	0.0002414	9.015271	1	-2	-3.109304
0.0002936	0.0002420	9.006682	1	2	1.624553
0.0002833	0.0002807	-5.368171e-2	0	25	1.557050

Table 5: Frequency analysis in the librational motion of Epimetheus.

Amp num (rad)	Amp ana (rad)	Freq (rad/days)	$\bar{n} - g_E$	ν	phase num (rad)
2.0123181	1.9944651	-2.147269e-3	0	1	1.557932
0.2308833	0.2288314	-6.441806e-3	0	3	1.532207
0.0733653	0.0727252	-1.073634e-2	0	5	1.506486
0.0663793	0.0776581	9.008825	1	1	1.480769
0.0661245	0.0769570	9.013120	1	-1	1.455058
0.0502353	0.0475310	9.015267	1	-2	-1.095877
0.0502025	0.0466766	9.006678	1	2	-2.193205
0.0337664	0.0334672	-1.503088e-2	0	7	1.429354
0.0329662	0.0304206	9.010973	1	0	1.403659
0.0184537	0.0182901	-1.932542e-2	0	9	1.377974
0.0140335	0.0169251	9.017414	1	-3	1.326685
0.0137124	0.0173919	9.004531	1	3	1.353514
0.0111480	0.0110491	-2.361996e-2	0	11	-0.230655
0.0071934	0.0071296	-2.791449e-2	0	13	-1.766568
0.0060059	0.0045923	9.002383	1	4	-1.836226
0.0058414	0.0044287	9.019562	1	-4	2.855327
0.0048634	0.0048203	-3.220903e-2	0	15	2.966333
0.0042848	0.0009103	9.021709	1	-5	-1.741864
0.0041635	0.0009525	9.000236	1	5	-1.860891

Eq. 4 to those obtained with our approach Eq. 31 is equal to $J_0(\beta_1)$. In the case of Janus, $J_0(\beta_1)$ is equal to 0.92 and for Epimetheus it is equal to 0.22. This explains why our results are consistent with the Tiscareno et al. (2009) results obtained for Janus, but depart from that study by a factor 4 for Epimetheus.

However for observations collected over short time spans (small with respect to the period of 8 years associated to the horseshoe orbit), the term νt is almost constant, and it is tempting to describe the motion of the short-period part of γ, denoted γ_s by a single sine term of frequency $\bar{n} - g$. In other words, it is possible to keep $\mathcal{B}_N(t)$ constant in the relations (18) and (20) and solve the equation of the rotation (19). Then we simply get:

$$\begin{aligned} \gamma_s =& \gamma_0 \sin((\bar{n} - g)t + \ell_0 + \mathcal{B}_N) \quad \text{with} \\ \gamma_0 =& \frac{2\bar{e}\bar{\sigma}^2}{\bar{\sigma}^2 - (\bar{n} - g)^2} \end{aligned} \tag{36}$$

It is worth mentioning that when ν tends toward zero in the solution (31), we get the previous expression of γ_s with $\mathcal{B}_N = \mathcal{B}_1$.

The approximation mentioned above becomes invalid for longer observation intervals (i.e., several years). Indeed, on a short time interval, $\mathcal{B}_N$ undergoes variations greater than 32° for Janus and 110° for Epimetheus. Consequently, if we try to express γ_s in terms of a periodic function at the orbital period $\bar{n} - g$, we obtain:

$$\begin{aligned} \gamma_s &= \gamma_0 \sin((\bar{n} - g)t + \ell_0 + \mathcal{B}_N(t)) \\ &= \gamma_0 A(t) \sin((\bar{n} - g)t + \ell_0) \\ &+ \gamma_0 B(t) \cos((\bar{n} - g)t + \ell_0) \end{aligned} \tag{37}$$

where $A(t) = \cos(\mathcal{B}_N(t))$ is time-dependent and where the out-of-phase term $B(t) = \sin(\mathcal{B}_N(t))$ is not small as shown in Figure 3 that presents the variations of these coefficients with time. For Janus, the in-phase term A varies between 0.84 and 1 (bold solid line) while B is in the interval $[-.52 : .52]$ (thin solid line). The variations are larger for Epimetheus, for which A (bold dashed line) fills the interval $[-1 : 1]$, and where B is greater than -0.8. As a consequence, the variations of $A(t)$ and $B(t)$, combined with the long-term behavior of the librational solution $\mathcal{B}_N$, have to be fitted explicitly in order to yield a robust determination of the rotational motions of Janus and Epimetheus. Using a single term $\gamma_0 \sin((\bar{n} - g)t + \ell_0)$ with γ_0 constant will overestimate or underestimate the librational amplitudes, depending on the date of the observations.

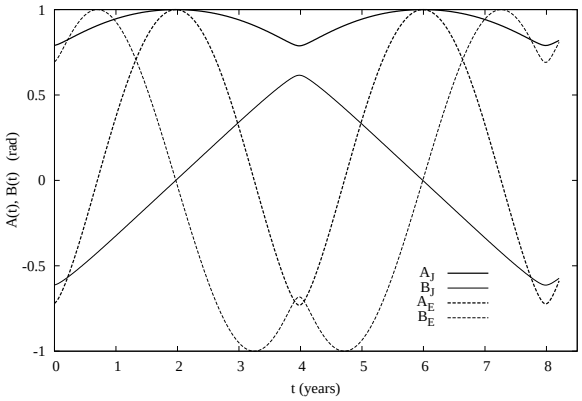

Figure 3: Temporal variations of the coefficients A and B involved in the equation (37). The solid lines correspond to Janus while the dashed lines represent Epimetheus.

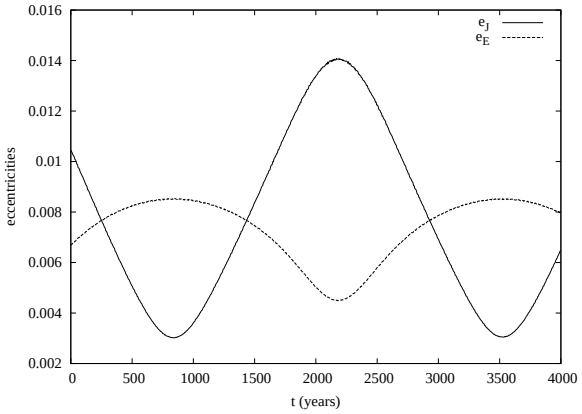

Figure 4: Secular variations of the eccentricities of the two satellites (solid curve for Janus, dashed curve for Epimetheus) due to their mutual gravitational interactions.

5.2 Long term variations of the eccentricities

The long-term variations of the eccentricities of the co-orbital satellites were introduced in Section 3.1. We now focus on these variations, which significantly influence the rotations of Janus and Epimetheus over the long term. The evolutions of the eccentricities are represented in Fig. 4. The main oscillation has a period of $2\pi/(g_J - g_E) = 4850$ years, according to Table 1. During the 400-year numerical integration, the variations of the eccentricities are significant (according to Fig. 4: e_J increases by $\sim$ 20%, while e_E decreases by more than 40%). Consequently, the amplitudes of the short-period librations, which are proportional to the eccentricities, are modulated with the same ratio. This time span being shorter than $1/12^{th}$ of the modulation period of the libration, γ cannot be recognized as a quasi-periodic function. In this situation, the frequency analysis method averages the long-period component of the signal (see Laskar 2005). For the purpose of validating the analytical approach, the eccentricities e of the satellites have been averaged $\bar{e}$ over 400 years. However, for data fitting, one should use the values of the eccentricities at the time of the observations.

5.3 Higher harmonics

Tiscareno et al. (2009) found in the shape fitting residuals an unexplained offset in the direction of the longest figure axis of the moons, constant in time, both for Janus (5.2 deg.) and Epimetheus (1 deg.). These authors interpreted these departures from the theoretical shape models by the presence of large density anomalies. We investigate such hypothesis by assuming that the satellites shapes depart from triaxial, hydrostatic shapes, due to topographic anomalies expressed at the third degree of spheric harmonics Williams et al. (2001)

$$\phi = \frac{\zeta(-15S_{33} + 0.5S_{31})}{\bar{\sigma}^2} \tag{38}$$

where $\zeta = 0.308$ rad/days^2 for Janus and 0.214 rad/days^2 for Epimetheus. Thus, the offset determined by Tiscareno et al. (2009) requires the $(-15S_{33} + 0.5S_{31})$ coefficient to be about 6.14 for Janus and 0.12 for Epimetheus. As a comparison, for the Earth's moon that coefficient has a value of 2.8 10^{-5}. Therefore, such gravity anomalies seem unrealistically large, even for rubble-piles like Janus and Epimetheus. Nevertheless, the contribution of density anomalies cannot be completely ruled out, and more complex shape models remain to be developed in order to better assess the influence of non-hydrostatic anomalies on rotation.

5.4 Tidal dissipation

The constant offset determined by Tiscareno et al. (2009) might result in tidal dissipation. The planet raises a tidal bulge on each moon that is shifted from the planet-satellite direction due to the inelastic response of planetary material. The gravitational torque exerted by Saturn on the permanent bulge will displace the rigid bulge to cancel the average saturnian torque acting on the tidal bulge.

The displacement is proportional to the ratio k_2/Q (see Williams *et al.* (2001) and Rambaux *et al.* (2010)). There are few constraints on the dissipation factors Q of porous bodies. In general, that dissipation factor is assumed to be 100. However there is no laboratory measurements supporting that choice, thus in the case of Janus and Epimetheus it is not obvious that these objects are even dissipative. Therefore, the value of 100 should be taken as a lowerbound.

The Love number k_2 depends on internal structure and therefore on the origin of the bodies. Charnoz (2009) (see also Charnoz *et al.* , 2009) suggested that many small satellites of Saturn, and especially Janus and Epimetheus, come from the accretion of ring material in the form of lumps that separate from the rings. We expect this accretion scenario to yield homogeneous satellites whose composition is mostly water ice. This corresponds to a porosity of about 30%, which might be uniform at the global scale. Assuming this model of formation, it is possible to compute k_2 using the McDonald (1964) equation for a homogeneous body. This parameter is a function of the satellite global shear modulus. The Youngs modulus of water ice with 30% porosity is about 3 GPa while its Poissons ratio is about 0.3 (Keller *et al.* 1999), which yields a shear modulus of about 1 GPa. We find $k_2 = 1.4\ 10^{-4}$ for Janus and $k_2 = 7\ 10^{-5}$ for Epimetheus. Consequently, by using the k_2 and $Q = 100$ the displacements of the axis of figure of Janus and Epimetheus are of the order of 0.014 deg for Janus and 0.026 deg for Epimetheus, which are too small to explain the offset Tiscareno et al. (2009).

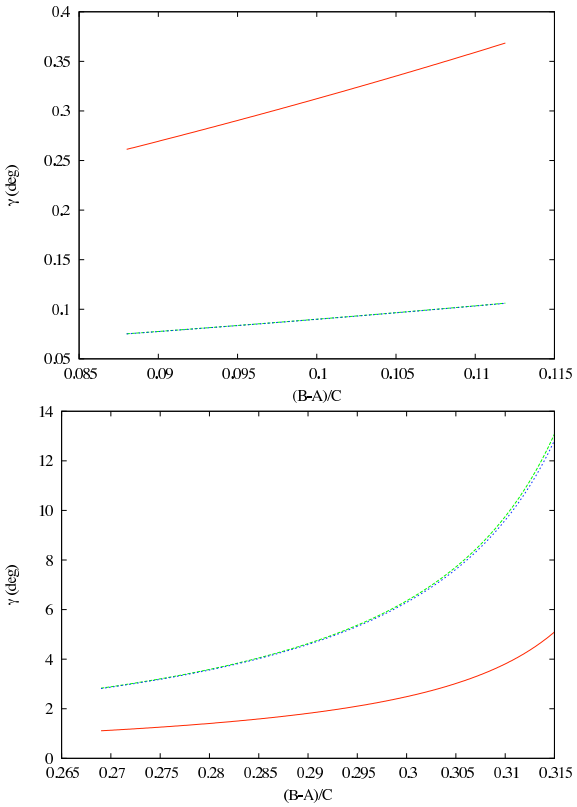

Figure 5: Influence of shape triaxiality on the mode $\bar{n} - g_k$ (red curve), where k is equal to J for Janus and E for Epimetheus, $\bar{n} - g_k + \nu$ (green curve), and $\bar{n} - g_k - \nu$ (blue) curve for Janus (a) and Epimetheus (b).

5.5 Influence of the triaxiality on the librational amplitudes

The short-period librations are of geophysical interest because their amplitudes depend on triaxiality, as shown in Eq. (31). We range the triaxiality inside the error bars provided by Tiscareno et al. (2009) for Janus 0.100 ± 0.012 and for Epimetheus $[0.269 : 0.315]$. For Janus, the libration amplitude depends linearly on triaxiality, while for Epimetheus this dependence is hyperbolic because the proper period and the orbital period are close to each

other (see Fig. 5).

The model suggested by Charnoz (2009) leads to homogeneous bodies. Alternatively, Porco et al. (2007) suggested that both satellites could have accreted rings particles around a core of satellite material with a lower porosity. This idea is supported by the fact that accretion models can account for the very oblate shapes of the satellites. That model implies a contrast in density between the core and a very porous outer layer. Porosity in that layer could be as large as 60 or 70%, as has been suggested for comets. There is little constraint on the thickness of that layer. Assuming Janus core is made up of solid, pure water ice, it would have a mean radius of about 70 km. Assuming an end-member model with a solid core of water ice and a 60% porous outer layer, decreases the mean moment of inertia by about 15% with respect to the value for a homogeneous body. Unfortunately, the size of the error bars on the triaxiality from Tiscareno et al. (2009) is of the order of 15%, which prevents further investigation of a possible relationship between libration amplitude and internal structure.

6 Conclusion

In this paper we have investigated the librational motion of the co-orbital satellites Janus and Epimetheus by using perturbative techniques and developing quasi-periodic solutions. For both satellites the solutions are composed of long-period librations linked to the orbital swap and short-period librations that bear the signature of the mass distributions in the satellites, and as such are means of investigating the internal structure of these objects.

We found that the amplitudes of the short-period librations depend on the magnitude of the forcing and the proximity to the resonance, as for the librations in a Keplerian framework, but also on Bessel functions of the longitudinal oscillations amplitudes. The latter term and librations at all harmonics have to be accounted for in order to properly reduce shape data and increase the robustness of the interpretation.

Acknowledgments

Part of this work has been conducted at the Jet Propulsion Laboratory, California Institute of Technology, under a contract with the National Aeronautics and Space Administration.

References

Charnoz, S. (2009). Physical collisions of moonlets and clumps with the Saturn's F-ring core. Icarus, 201:191–197.

Charnoz, S., Salmon, J., Crida, A., Brahic, A. (2009). Origin and Evolution of Saturn's Small Satellites. Bull. American Astronomical Society, 52.08.

Dermott, S. F. and Murray, C. D. (1981). The dynamics of tadpole and horseshoe orbits II. The coorbital satellites of saturn. Icarus, 48:12–22.

Giorgini, J. D., Yeomans, D. K., Chamberlin, A. B., Chodas, P. W., Jacobson, R. A., Keesey, M. S., Lieske, J. H., Ostro, S. J., Standish, E. M., and Wimberly, R. N. (1996). JPL's On-Line Solar System Data Service. In Bulletin of the American Astronomical Society, volume 28 of Bulletin of the American Astronomical Society, page 1158.

Greenberg, R. (1981). Apsidal precession of orbits about an oblate planet. Astron. J., 86:912–914.

Jacobson, R. A., Spitale, J., Porco, C. C., Beurle, K., Cooper, N. J., Evans, M. W., and Murray, C. D. (2008). Revised Orbits of Saturn's Small Inner Satellites. Astron. J., 135:261–263.

Keller, T., Motschmann, U., Engelhard, L. (1999), Modelling the poroelasticity of rocks and ice. Geophysical Prospecting, 47, 509–526.

Laskar, J. (1988). Secular evolution of the solar system over 10 million years. Astron. Astrophys., 198:341–362.

Laskar, J. (2005). Frequency map analysis and quasiperiodic decomposition. In Benest, D., editor, Hamiltonian systems and Fourier analysis : new prospects for gravitational dynamics, Advances in astronomy and astrophysics, pages 99–129. Cambridge Scientific Publishers.

McDonald, G. J. F. (1964). Tidal Friction. Rev. Geophys., 2:467–541.

Murray, C. D. and Dermott, S. F. (1999). Solar System Dynamics. Cambrige univ. press.

Namouni, F. (1999). Secular Interactions of Coorbiting Objects. Icarus, 137:293–314.

Noyelles, B. (2010). Theory of the rotation of Janus and Epimetheus. ArXiv e-prints.

Porco, C. C., Thomas, P. C., Weiss, J. W., Richardson, D. C. (2007). Saturns Small Inner Satellites: Clues to Their Origins. Science, 318:1602–1605.

Rambaux, N., Castillo-Rogez, J. C., Williams, J.G., Karatekin, Ö. (2010). The librational response of Enceladus. Geophys. Res. Lett., in press.

Tiscareno, M. S., Thomas, P. C., and Burns, J. A. (2009). The rotation of Janus and Epimetheus. Icarus, 204:254–261.

Williams, J. G., Boggs, D. H., Yoder, C. F., Ratcliff, J. T., and Dickey, J. O. (2001). Lunar rotational dissipation in solid body and molten core. Journal of Geophysical Research, 106:27933–27968.

Yoder, C. F., Colombo, G., Synnott, S. P., and Yoder, K. A. (1983). Theory of motion of Saturn's coorbiting satellites. Icarus, 53:431–443.

A Development in Bessel functions

The Bessel functions can be defined as Fourier's coefficients of the 2π-periodic function $u \longmapsto e^{ix\sin u}$ where x is a real parameter, that is:

$$e^{ix\sin u} = \sum_{k=-\infty}^{+\infty} J_k(x) e^{iku}$$

$$\text{with} \quad J_k(x) = \frac{1}{2\pi}\int_0^{2\pi} \exp i(x\sin u - ku)du = \frac{1}{2\pi}\int_0^{2\pi} \cos(x\sin u - ku)du$$

These functions satisfy the two following relations that we use in Section 4.1.1 :

$$\text{for all } p \in \mathbb{N}, \quad J_{-p}(x) = (-1)^p J_p(x)$$

$$\text{for all } p \in \mathbb{N}, \quad J_p(x) = \frac{x^p}{2^p p!}(1 + O(x^2))$$

In addition, we show in Tables 6 and 7 the values of the main coefficients $J_q(\beta_p)$ that are greater than $1.\,10^{-6}$. This tables are useful to evaluate the accuracy of our analytical solution (see Section 4.2), and also to identify terms capable of increasing the accuracy of the solution.

B Table of definition of variables

Table 6: Numerical values of the coefficients $J_q(\beta_p)$ in the case of Janus. The "−" symbol indicates that the corresponding value is lower than $1.\,10^{-6}$.

p	$J_0(\beta_p)$	$J_1(\beta_p)$	$J_2(\beta_p)$	$J_3(\beta_p)$	$J_4(\beta_p)$	$J_5(\beta_p)$
1	0.92488	0.26626	0.03732	0.00346	0.00024	0.00001
3	0.99899	0.03173	0.00050	-	-	-
5	0.99990	0.01009	0.00005	-	-	-
7	0.99998	0.00464	0.00001	-	-	-
9	0.99999	0.00254	-	-	-	-
11	1.00000	0.00153	-	-	-	-
13	1.00000	0.00099	-	-	-	-
15	1.00000	0.00067	-	-	-	-
17	1.00000	0.00047	-	-	-	-
19	1.00000	0.00034	-	-	-	-
21	1.00000	0.00025	-	-	-	-
23	1.00000	0.00018	-	-	-	-
25	1.00000	0.00014	-	-	-	-
27	1.00000	0.00011	-	-	-	-
29	1.00000	0.00008	-	-	-	-
31	1.00000	0.00007	-	-	-	-
33	1.00000	0.00005	-	-	-	-
35	1.00000	0.00004	-	-	-	-
37	1.00000	0.00003	-	-	-	-
39	1.00000	0.00003	-	-	-	-

Table 7: Numerical values of the coefficients $J_q(\beta_p)$ in the case of Epimetheus

p	$J_0(\beta_p)$	$J_1(\beta_p)$	$J_2(\beta_p)$	$J_3(\beta_p)$	$J_4(\beta_p)$	$J_5(\beta_p)$
1	0.22708	0.57708	0.35159	0.12806	0.03366	0.00695
3	0.98695	0.11367	0.00652	0.00025	-	-
5	0.99868	0.03634	0.00066	-	-	-
7	0.99972	0.01673	0.00014	-	-	-
9	0.99992	0.00914	0.00004	-	-	-
11	0.99997	0.00552	0.00002	-	-	-
13	0.99999	0.00356	-	-	-	-
15	0.99999	0.00241	-	-	-	-
17	1.00000	0.00169	-	-	-	-
19	1.00000	0.00121	-	-	-	-
21	1.00000	0.00089	-	-	-	-
23	1.00000	0.00067	-	-	-	-
25	1.00000	0.00051	-	-	-	-
27	1.00000	0.00039	-	-	-	-
29	1.00000	0.00030	-	-	-	-
31	1.00000	0.00024	-	-	-	-
33	1.00000	0.00019	-	-	-	-
35	1.00000	0.00015	-	-	-	-
37	1.00000	0.00012	-	-	-	-
39	1.00000	0.00010	-	-	-	-

Table 8: Definition of main variables used in the paper

μ	=	Constant of the third Kepler law
J_2	=	Oblateness of Saturn
M_i	=	Mass of the body where the subscript i characterized the body
ζ_i	=	reduced mass $(m_i/(m_J + m_E))$
R_i	=	Radius of the body where the subscript i characterized the body
I	=	the inertia tensor.
A, B, C	=	Normalized $(M_i R_i 2)$ moments of inertia of the whole planet $(A < B < C)$.
θ	=	Rotation angle defined as the angle between the orientation of the principal axes A and the line of node of the orbit.
γ	=	physical libration, oscillation around a mean uniform motion.
ℓ	=	Mean Anomaly
f	=	True Anomaly
λ	=	mean longitude of the orbit
λ_r	=	relative mean longitude $(\lambda_J - \lambda_E)$
β_i	=	Amplitude of the expanding series of λ
v	=	draconic true longitude of the orbit $(f + \omega)$
ω	=	argument of pericenter
ϖ	=	longitude of pericenter
Ω	=	longitude of ascending node
a	=	semi-major axis.
$\bar{a}$	=	mean semi-major axis (iterative computation)
a_r	=	relative semi-major axis $(a_J - a_E)$
α_i	=	Amplitude of the expanding series of a
e	=	eccentricity.
$\bar{e}$	=	mean eccentricity
g	=	frequency of the longitude of pericenter (ϖ).
s	=	frequency of the node (Ω).
$\bar{n}$	=	mean mean motion (λ)
ν	=	orbital libration frequency.
σ	=	spin-orbit libration frequency.
$\bar{\sigma}$	=	mean spin-orbit libration frequency.